UNIVERSIDAD CARLOS III DE MADRID working papers

UC3M Working Papers
Statistics and Econometrics
16-09
ISSN 2387-0303
Julio 2016

Departamento de Estadística
Universidad Carlos III de Madrid
Calle Madrid, 126
28903 Getafe (Spain)
Fax (34) 91 624-98-48

Monitoring variance by EWMA charts with time varying smoothing parameter

Willy Ugaz[a,*], Andrés M. Alonso[a] and Ismael Sánchez[a]

Abstract

Memory charts like EWMA-S^2 or CUSUM-S^2 can be designed to be optimal to detect a specific shift in the process variance. However, this feature could be a serious inconvenience since, for instance, if the charts are designed to detect small shift, then, they can be inefficient to detect moderate or large shifts. In the literature, several alternatives have been proposed to overcome this limitation, like the use of control charts with variable parameters or adaptive control charts. This paper proposes new adaptive EWMA control charts for the dispersion (AEWMA-S^2) based on a time-varying smoothing parameter that takes into account the potential misadjustment in the process variance. The obtained control charts can be interpreted as a combination of EWMA control charts designed to be efficient for different shift values. Markov chain procedures are established to analyse and design the proposed charts. Comparisons with other adaptive and traditional control charts show the advantages of the proposals.

Keywords:

Adaptive control charts, Average Run Length, EWMA, CUSUM, Statistical Process Control.

[a] Department of Statistics, Universidad Carlos III de Madrid.
[a,*] Corresponding autor.

Acknowledgements: financial support from the Spanish Ministry of Education and Science, research project ECO2012-38442.

Monitoring variance by EWMA charts with time varying smoothing parameter

Willy Ugaz, Andrés M. Alonso and Ismael Sánchez*

Universidad Carlos III de Madrid

July 20, 2016

Abstract

Memory charts like EWMA-S^2 or CUSUM-S^2 can be designed to be optimal to detect a specific shift in the process variance. However, this feature could be a serious inconvenience since, for instance, if the charts are designed to detect small shift, then, they can be inefficient to detect moderate or large shifts. In the literature, several alternatives have been proposed to overcome this limitation, like the use of control charts with variable parameters or adaptive control charts. This paper proposes new adaptive EWMA control charts for the dispersion (AEWMA-S^2) based on a time-varying smoothing parameter that takes into account the potential misadjustment in the process variance. The obtained control charts can be interpreted as a combination of EWMA control charts designed to be efficient for different shift values. Markov chain procedures are established to analyze and design the proposed charts. Comparisons with other adaptive and traditional control charts show the advantages of the proposals.

Keywords: Adaptive control charts, Average Run Length, EWMA, CUSUM, Statistical Process Control.

Address: Willy Ugaz, Andrés M. Alonso and Ismael Sánchez, Department of Statistic; Universidad Carlos III de Madrid; Avd. de la Universidad 30, 28911, Leganés, Madrid (Spain). email: wugaz@est-econ.uc3m.es, amalonso@est-econ.uc3m.es and ismael@est-econ.uc3m.es.

1 Introduction

The use of control charts as a process monitoring tool has become increasingly popular in the field of statistical process control (SPC). Shewhart control charts (Shewhart, 1931) can be used for monitoring the mean or the variability of the process. In many practical applications, it is even more important to control shifts in the process variability rather than the mean, since an increase of the variability process causes an increased number of defective products while a decrease of process variability implies an improvement of process capability (Acosta-Mejia et al., 1999). Besides, it is meaningless to claim a shift of the process mean unless it is sure that the process variability is in control.

Shewhart control charts such as the range R or the unbiased sample variance S^2 control charts can be used for monitoring the variability of rational subgroups sampled of the process. However, as in the case of monitoring the process mean, these procedures are not very sensitive to small shifts.

In order to increase the sensitivity to small shifts, the literature has proposed some alternative procedures that use statistics with memory, usually called memory control charts or time-weighted control charts. It is known that the most popular memory control charts are the CUSUM and the EWMA charts, which have been recognized as potentially powerful tools in quality control. One of the first CUSUM control charts for monitoring variability was introduced by Page (1963) and then studied, among others, by Bagshaw and Johnson (1975), Hawkins (1981), Box and Ramírez (1991), Chang and Gan (1995), Castagliola et al. (2009) and Nazir et al. (2015).

Furthermore, Wortham and Ring (1971), Sweet (1986) and Ng and Case (1989) investigated the properties of EWMA control charts for monitoring the process variability but they were not able to introduce formal design strategies for the problem. Box, Hunter and Hunter (1978), among others, introduced the use of the logarithm of the sample variances since it is more approximately normally distributed than the sample variance by itself. Crowder and Hamilton (1992) proposed an EWMA control chart for monitoring the variability based on the logarithmic transformation of the sample variance, $\log\left(S^2\right)$, due to its simplicity and efficiency. Castagliola (2005) proposed a bilateral EWMA control chart for monitoring the variability using a logarithmic transformation of three parameters (type of original Johnson (1949) transformations) to improve normality.

As an extension of the Crowder and Hamilton (1992) proposal, Shu and Jiang (2008) presented an EWMA control chart for monitoring the variability (NEWMA), which truncates the negative normalized observations to zero in the statistical traditional EWMA. Maravelakis and Castagliola (2009) propose a modified EWMA control chart for monitoring the standard deviation when the parameters are estimated. Castagliola et al. (2010) presented an EWMA control chart that improves the 2005 version. This chart uses the Johnson transformation of four parameters to attain normality.

Other interesting researches that study CUSUM and EWMA control charts for the process variability can be found in Tuprah and Ncube (1987), MacGregor and Harris (1993), Gan (1995), Lowry et al. (1995), Acosta-Mejia (1998), Amin et al. (1999), Chao-Wen and Reynolds (1999), Acosta-Mejía et al. (1999), Huwang et al. (2010), Abbasi (2010), Abbasi and Miller (2013) and Haq et al. (2014), among others.

Also, with the aim of improving the performance, Interval Sampling Variable (VSI) and Sample Size Variable (VSS) EWMA control charts for the process variability have been proposed by Castagliola et al. (2006, 2008). Other contributions can be seen in Chengular et al. (1989) and Reynolds and Stoumbos (2001).

Analogously to the control of the process mean, adaptive CUSUM and EWMA control charts for monitoring the variability process can be proposed based on time-varying versions of the parameters that control the memory of the charts; that is k in CUSUM charts and λ in EWMA charts. By adapting the memory, we can make charts sensitive to both small and large shifts. The intuition behind these adaptive charts is to use a measure of the potential presence of a shift. Accordingly, the value of the parameter is increased when it is suspected that the process could be out of control due to a large shift. Conversely, if the data show strong evidence of being in control or with a small shift, the parameters tend to be smaller, easing the detection of potential small shifts. This kind of adaptation scheme is the one we pursue in this paper.

Shu et al. (2010) proposed an adaptive CUSUM control chart for monitoring shifts in the process variability (ACUSUM-S^2). This chart is an extension of the ACUSUM control chart for monitoring the process mean initially proposed by Sparks (2000). This ACUSUM-S^2 chart dynamically adjusts its reference value according to a current estimate of the process variance and does not require precise information about the magnitude of shift.

Capizzi and Masarotto (2003) developed an AEWMA control chart for monitoring the process mean based on weighting recent observations using an score function of the current error $e_t = x_t - y_{t-1}$, where x_t is the last observation of the process and y_{t-1} is the previous value of the monitoring statistic. In particular, if e_t is small, the value of λ tends to be small, like in conventional EWMA chart, since the process seems to be in control. However, if e_t is large the value of λ tends to be large, since the risk of being out of control is higher.

Shu (2008), considering the statistic of Crowder and Hamilton (1992), proposed an adaptive EWMA control chart for monitoring the process variability. This chart is based on the latest observations dynamically weighted according to an appropriate function of the current prediction error. It is actually an extension of Capizzi and Masarotto (2003) for monitoring the process mean.

Additionally, some new AEWMA control charts for monitoring the process mean are proposed by Ugaz et al. (2016). These charts use specific statistics that quantify the evidence of a shift from data, that is, statistics based on the distance from observations x_t to the process mean μ_0 or based on the prediction error, e_t, or just based on the level of y_{t-1}. Subsequently, the statistics are translated to time varying smoothing factor λ_t. Those AEWMA control charts are competitive with respect to the proposal of Capizzi and Masarotto (2003).

In this paper, considering the proposals of Ugaz et al. (2016), some alternative AEWMA-S^2 control charts are proposed. To that aim, several measures of the potential shift of the process variance are suggested. For each measure of potential shift, alternative methods to translate such measure into a time varying smoothing factor are discussed. Procedures to compute the ARL of the proposed AEWMA-S^2 based on Markov chain approximations are obtained, which allow us to get the optimal designs. A numerical comparison of these alternative approaches and the main alternatives in the literature is presented.

The rest of the article is organized as follows. In Section 2, the notion of the adaptive EWMA-S^2 control chart is introduced. In Section 3, AEWMA-S^2 control charts with time varying λ_t based on the last observation are proposed. In Section 4, AEWMA-S^2 control charts with time varying λ_t based on the level of the control statistics are proposed. Section 5, shows the results of several comparisons between alternative control charts and the proposed AEWMA-S^2 control charts. Finally, in Section 6, some concluding remarks are given.

2 Adaptive EWMA-S^2 control chart

Assume that observations $X_{t,i}$, $t = 1, 2, \cdots$ and $i = 1, 2, \cdots, n$ are independent and identically distributed following a normal distribution $N\left(\mu, \sigma_t^2\right)$. Furthermore, we are mainly interested in detecting increases in the process variance, i. e., $\sigma_t^2 = \sigma_0^2, t < t^*$ and $\sigma_t^2 > \sigma_0^2, t \geq t^*$ and $\tau_t = \sigma_t/\sigma_0$. Let S_t^2 be the variance of the $t-$th rational subgroup of size n defined by $S_t^2 = \left(1/\left(n-1\right)\right)\sum_{i=1}^{n}\left(X_{t,i} - \overline{X}_t\right)^2$, where $X_{t,i}$ is the $i-$th observation of the $t-$th rational subgroup and $\overline{X}_t$ is the $t-$th subgroup mean. Crowder and Hamilton (1992) suggested the EWMA chart for monitoring increases in the process variance with the statistic,

$$y_t = \max\left[0, \lambda M_t + \left(1-\lambda\right) y_{t-1}\right], \quad y_0 = 0, \tag{1}$$

where $M_t = \ln\left(S_t^2/\sigma_0^2\right)$, which is more approximately normal distributed (Shu and Jiang, 2008). The mean and variance of the transformed variable M_t are approximated by,

$$\mu_{_{M_t}} = \ln\left(\tau_t^2\right) - \frac{1}{n-1} - \frac{1}{3\left(n-1\right)^2} + \frac{2}{15\left(n-1\right)^4}, \tag{2}$$

and

$$\sigma^2_{M_t} = \frac{2}{n-1} + \frac{2}{(n-1)^2} + \frac{4}{3\,(n-1)^3} - \frac{16}{15\,(n-1)^5}, \tag{3}$$

respectively. It is important to note that $\sigma^2_{M_t}$ only depends on n, it is because of that M_t can be monitored as X_t in the EWMA chart for monitoring the process mean. This EWMA-S^2 control chart signals when,

$$y_t > h, \tag{4}$$

where h is a threshold that determines the ARL_0.

To design the EWMA-S^2 control chart for the variance process (EWMA-S^2), the parameter values of λ and h for some rational subgroup of size n must be selected. λ and h, which are defined in (1) and (4) can be chosen in such a way that the chart is optimal for detecting a prespecified shift in the variance process for a given in control average run length (ARL_0). The influence of the design parameters in the performance of the EWMA-S^2 has been studied by Box, Hunter and Hunter (1978), Crowder and Hamilton (1992), Castagliola (2005), Shu and Jiang (2008), Castagliola et al. (2010), Huwang et al. (2010), Abbasi (2010) among others.

The ARL of this AEWMA-S^2 is a function of the shift, $\tau = \sigma_1/\sigma_0$ (σ_0 is the standard deviation of the in control process and σ_1 is the standard deviation of process when it is out of control), λ, h and n. It can be written as ARL=ARL$(\lambda, h|\tau, n)$. Then, by solving the following optimization problem, the optimal values of λ and h that minimize the ARL$(\lambda, h|\tau, n)$ can be obtained:

$$\begin{aligned} &\min_{\lambda,h} \left(ARL\left(\lambda, h|\tau, n\right)\right) \\ &\text{subject to:} \\ &ARL\left(\lambda, h|\tau = 1, n\right) = ARL_0, \end{aligned}$$

where, depending on the EWMA-S^2 proposals, the $ARL\left(\lambda, h|\tau \neq 1, n\right)$ can be approximated by a discrete Markov chain procedure.

Whereas an optimal EWMA-S^2 chart would need a different value of λ for each τ, the same value of λ can be a reasonable option for some range of shifts. However, there is not a single value of λ that can provide optimal or nearly optimal EWMA charts for both small and large values of τ. To illustrate this fact, we have calculated the optimal design for each shift τ, for $\text{ARL}_0 = 200$ and $n = 5$, using the proposal of Crowder and Hamilton (1992) with the transformation M_t. The optimal λ is denoted as λ^* and the minimum ARL is denoted as ARL*. Figure 1-a shows the comparison between the optimal design for ARL* and the range of designs with $ARL \leq 1.1 \times ARL^*$ That is, we find the optimal design for each shift as well as those designs that are nearly optimal in the sense that their ARL in each shift is not larger than a 10% of the minimum one.

Table 1 and Figure (1-b) shows the range $[\lambda_1, \lambda_2]$ of λ for which the value of ARL varies in the range $[ARL^*, 1.1 \times ARL^*]$. For example, if $\lambda = 0.15$, it possible to get acceptable values of ARL (with a difference lower than 10% of ARL^*) for small shifts from $\tau \approx 1.1$ to 1.5. If $\lambda = 0.7$, it is possible to get acceptable values of ARL for $\tau \geq 1.4$. Table 1 shows that, for instance, if $\tau = 1.3$ then it is possible to get an $ARL \in [10.52, 11.57]$ for a $\lambda \in [0.005, 0.5703]$. When the shift is small, for instance, $\tau \in (1, 1.4]$, it can be seen that the differences between the ARL^* and $1.1 \times ARL^*$ are notable and therefore the variation of λ has large influence in the ARL. Conversely, for $\tau \geq 1.5$, the influence of λ in ARL is small.

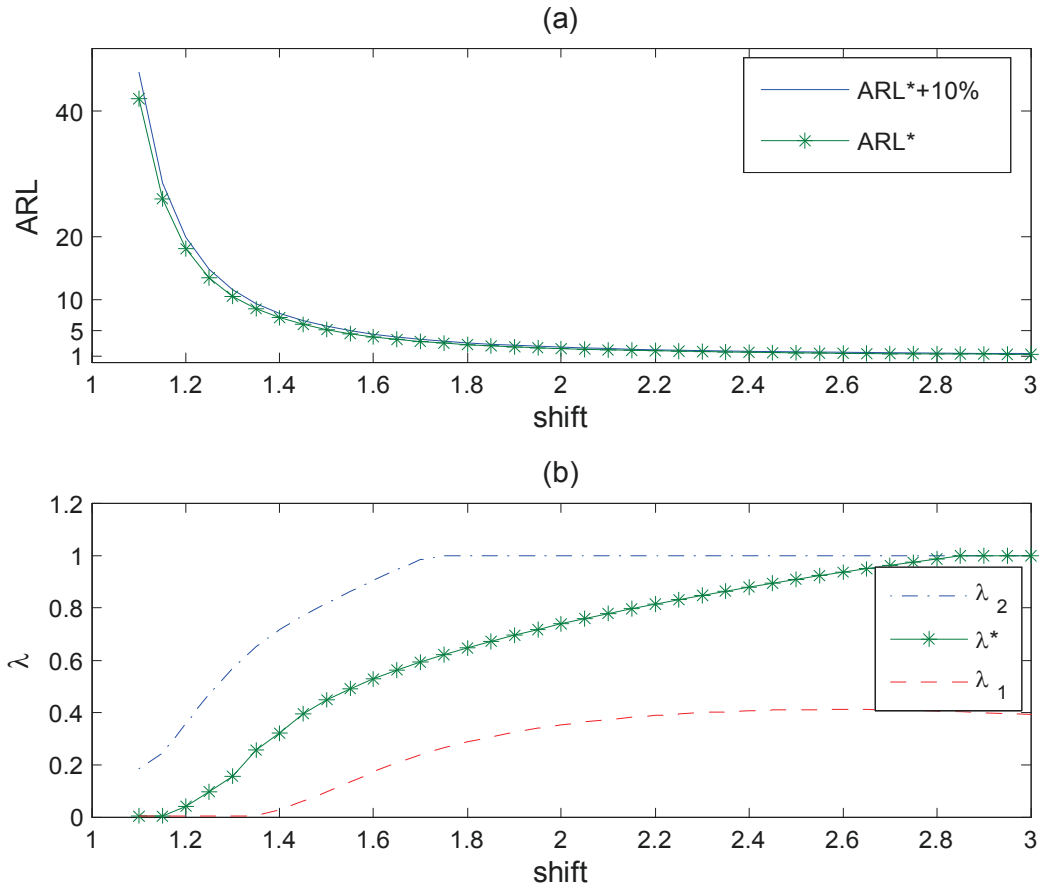

Figure 1: (a) Comparison between the ARL^* (–∗–) and $ARL^* + 10\% \times ARL^*$ (—). (b) λ^* behavior (–∗–), and a range of variation defined by λ_1 (– –) and λ_2 (–·–).

As a conclusion, if we want an EWMA-S^2 with a good performance for all shifts, we need to use a time varying λ, that is $\lambda = \lambda_t$. The above results suggest that λ_t must depend on the shift. But, in real situations, the shift is unknown and we need to find measures of the evidence of shift based on the data. Those measures will be translated to an appropriate value λ_t. If data suggest that the process dispersion could be shifting, the value of λ_t would increase to allow y_t to be closer to the new variance.

τ	λ^*	$\mathbf{ARL}^*$	$1.1 * \mathbf{ARL}^*$	$[\lambda_1, \lambda_2]$
1.1	0.005	41.98	46.18	[0.005, 0.187]
1.2	0.042	18.09	19.90	[0.005, 0.356]
1.3	0.157	10.52	11.57	[0.005, 0.570]
1.4	0.321	7.08	7.78	[0.030, 0.717]
1.5	0.449	5.18	5.70	[0.098, 0.819]
1.6	0.529	4.04	4.45	[0.173, 0.905]
1.7	0.593	3.31	3.64	[0.239, 0.986]
1.8	0.648	2.80	3.08	[0.289, 1.000]
1.9	0.696	2.44	2.69	[0.326, 1.000]
2.0	0.739	2.17	2.39	[0.354, 1.000]
2.1	0.778	1.97	2.17	[0.374, 1.000]
2.2	0.814	1.81	1.99	[0.389, 1.000]
2.3	0.848	1.68	1.85	[0.400, 1.000]
2.4	0.879	1.58	1.74	[0.407, 1.000]
2.5	0.909	1.50	1.65	[0.410, 1.000]
2.6	0.937	1.43	1.57	[0.411, 1.000]
2.7	0.963	1.37	1.51	[0.409, 1.000]
2.8	0.988	1.32	1.46	[0.405, 1.000]
2.9	1.000	1.28	1.41	[0.399, 1.000]
3.0	1.000	1.25	1.38	[0.392, 1.000]

Table 1: Minimum ARL for each shift τ and the corresponding λ .

This situation would facilitate to trigger the alarm. In the other hand, if data show low evidence of being shifting, a lower value would be fixed to the parameter λ_t This situation would facilitate the detection of a possible small shift.

In this regard, Capizzi and Masarotto (2003) propose an adaptive EWMA control chart (AEWMA) based on the behavior of data for monitoring the process mean. Later, and following the work of Crowder and Hamilton (1992) and Capizzi and Masarotto (2003), Shu (2008) presents an adaptive EWMA control chart for monitoring increases in the process variance (AEWMA-S^2) which considers the following statistic

$$y_t = \max\left[0, y_{t-1} + \phi\left(e_t\right)\right], \quad y_0 = 0, \tag{5}$$

where, $e_t = M_t - y_{t-1}$, M_t is defined in (1) and $\phi\left(e_t\right)$ is a score function based on Huber function (Huber, 1981),

$$\phi\left(e\right) = \begin{cases} e + \left(1-\lambda\right)\gamma & \text{if } e < -\gamma \\ \lambda e & \text{if } |e| \leq \gamma \\ e - \left(1-\lambda\right)\gamma & \text{if } e > \gamma \end{cases}, \tag{6}$$

where, γ is an additional parameter of the chart. Indeed, a signal of upward shift is issued when $y_t > h$, where h is a threshold that determines the ARL_0. A similar procedure could be followed if we

are interested in monitoring decreases in the process variance.

In this article we will analyze alternative strategies to get AEWMA-S^2 control charts using time-varying smoothing parameters, based on Ugaz et al. (2015), for monitoring increases in the process variance using the statistic,

$$y_t = \max\left[0, \lambda_t M_t + (1-\lambda_t)\, y_{t-1}\right], \qquad y_0 = 0, \tag{7}$$

where, M_t is the transformed variable by Crowder and Hamilton (1992). The alarm is triggered as soon as $y_t > h$, where h is a threshold that determines the ARL_0. We propose four different statistics for quantifying the evidence of a shift from data; we analyze several transformations that translate those statistics into a value for λ_t. The calculation of the ARL of the proposed adaptive control charts is approximated by Markov chain approach (Brook and Evans, 1972 and Lucas and Saccucci, 1990). Then, this ARL approximation is used to get optimal parameters for a given ARL$_0$. This Markov chain representation is used to optimize the parameters such that minimum ARL is attained for a given ARL$_0$.

3 AEWMA charts with λ_t based on the last M_t

In this section, we present several proposals for measuring the evidence of the shift in the process variance based on the last transformed variable M_t. The first proposal, denoted as AEWMA1-S^2, is based on the standardized distance from M_t to the target μ_{M0}. The second proposal, denoted as AEWMA2-S^2, is based on the standardized distance from M_t to the last value of the monitoring statistics, y_{t-1}. And finally, the third proposal is a combination of the previous proposals and it is denoted by AEWMA3-S^2. Then, the smoothing parameter λ_t is obtained by using a transformation of those three distances.

3.1 The AEWMA1-S^2 chart

This adaptive control chart uses the following statistic

$$T_{1t} = \left(\frac{M_t - \mu_{M0}}{\sigma_M}\right)^2, \tag{8}$$

as a measure of the evidence of the shift. Notice that T_{1t} is the standardized distance from the last transformed variable M_t to the target μ_{M0} and it tends to be larger in presence of a shift in the process variance. The terms μ_{M0} and σ_M are obtained by the expressions (2) and (3) when $\tau = 1$. Given y_{t-1}, the value of M_t is a random variable and it is approximately normal distributed (Shu and

Jiang, 2008). Therefore, If the process is in control, it holds that T_{1t} follows approximately a central chi-square distribution of one degree of freedom, χ^2_1. The cumulative distribution function is given by,

$$F_{1t} = P\left(\chi^2_1 \leq T_{1t}\right). \tag{9}$$

Although F_{1t} is a natural choice for λ_t since $F_{1t} \in [0,1]$ and it is an increasing function on T_{1t}, Sánchez (2006) has shown that the variability of F_{1t} can be very large, provoking a large variance of the monitoring statistics y_t. Then, some efficient transformation that translate F_{1t} into a smoothing parameter λ_t are required. In Ugaz et al. (2016), the following transformations have been explored:

- Linear bounded transformation

$$\lambda^{(1)}_{1t} = \lambda_{\min} + (\lambda_{\max} - \lambda_{\min})\, F_{1t}, \tag{10}$$

  where $\lambda_{\min}$ and $\lambda_{\max}$ are parameters that are optimized to attain the lowest ARL for a given ARL_0, and computed with a procedure described in subsection 3.4.

- Power transformation

$$\lambda^{(2)}_{1t} = \lambda_{\min} + (\lambda_{\max} - \lambda_{\min})\, F^a_{1t}, \tag{11}$$

  where a is another parameter to be optimized together with $\lambda_{\min}$ and $\lambda_{\max}$.

- Threshold transformation

$$\begin{aligned} \lambda^{(3)}_{1t} &= \lambda_{\min} + (\lambda_{\max} - \lambda_{\min})\, q_{1t}, \\ q_{1t} &= \begin{cases} 0 & \text{if} \quad F^a_{1t} \leq p_0, \\ \dfrac{F^a_{1t} - p_0}{1 - p_0} & \text{otherwise}, \end{cases} \end{aligned} \tag{12}$$

  where the threshold p_0 is a constant to be optimized together with a, $\lambda_{\min}$, and $\lambda_{\max}$.

It could be noticed that $\lambda_t = \lambda_{\min}$ when F^a_{1t} is smaller than prespecified threshold, p_0 (an percentile). Consequently, we will maintain a low smoothing factor unless the evidence of shift is large. If $F_{1t} > p_0$, we maintain a similar transformation as in (11) in such a way that the whole transformation is continuous. Moreover, the power transformation is a particular case of the threshold transformation when $p_0 = 0$ and the linear bounded transformation is a particular case of the power transformation when $a = 1$. Figure 2 shows two examples of how the value M_t is translated into a smoothing factor λ_t, with $\lambda_t = \lambda^{(3)}_{1t}$ in (12) for a particular AEWMA1-S^2 design. Without loss of generality, in this Figure 2 and Figures 3, 4 and 5, we are assuming that $X_t \sim N(0,1)$),

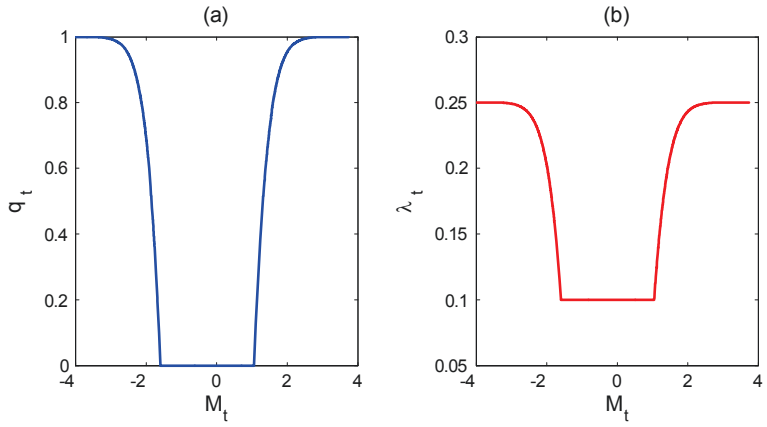

Figure 2: (a) Behavior of q_t in terms of M_t. (b) Behavior of λ_t parameter in terms of behavior M_t. It is considered a particular parameters set (PS), PS1: $\lambda_{\min} = 0.1$, $\lambda_{\max} = 0.25$, $a = 1$, $p_0 = 0.9$, and $h = 0.3031$.

3.2 The AEWMA2-S^2 chart

This adaptive control chart uses the following statistic

$$T_{2t} = \left(\frac{M_t - y_{t-1}}{\sigma_M} \right)^2, \tag{13}$$

as a measure of the evidence of the shift. Notice that T_{2t} is difference between the current M_t and the value of the AEWMA statistic in the previous time, y_{t-1}.and it tends to be larger in presence of a shift in the process variance. This statistic holds that

$$T_{2t} = \left(\frac{M_t - \mu_{M0}}{\sigma_M} + \frac{\mu_{M0} - y_{t-1}}{\sigma_M} \right)^2 = \left(Z_t + \frac{\mu_{M0} - y_{t-1}}{\sigma_M} \right)^2, \tag{14}$$

where Z_t is approximately a standard normal random variable (see Shu and Jiang, 2008). Given y_{t-1}, T_{2t} could be approximated by a non-central chi-square distribution of one degree of freedom, $\chi^2_1(\gamma_t)$, with noncentrality parameter $\gamma_t = (\mu_{M0} - y_{t-1})/\sigma_M$. As mentioned in Ugaz et al. (2016), the noncentrality parameter, γ_t, can be neglected for practical purposes. Thus, for the sake of simplicity, the transformation of T_{2t} into a smoothing parameter will be done by,

$$\begin{aligned} \lambda_{2t} &= \lambda_{\min} + (\lambda_{\max} - \lambda_{\min})\, q_{2t}, \\ q_{2t} &= \begin{cases} 0 & \text{if} \quad G^a_{2t} \le p_0, \\ \dfrac{G^a_{2t} - p_0}{1 - p_0} & \text{otherwise}, \end{cases} \\ G_{2t} &= P(\chi^2_1 \le T_{2t}), \end{aligned} \tag{15}$$

where the parameters $\lambda_{\min}$, $\lambda_{\max}$, p_0, and a, are optimized to minimize the ARL when the process is out of control, for a given ARL_0 using the procedure shown in subsection 3.4. Figure 3 illustrates how

λ_{2t} varies as a function of M_t, with two particular parameter sets. Since the statistics T_{2t} depend on y_{t-1} two curves with different values of y_{t-1} are displayed.

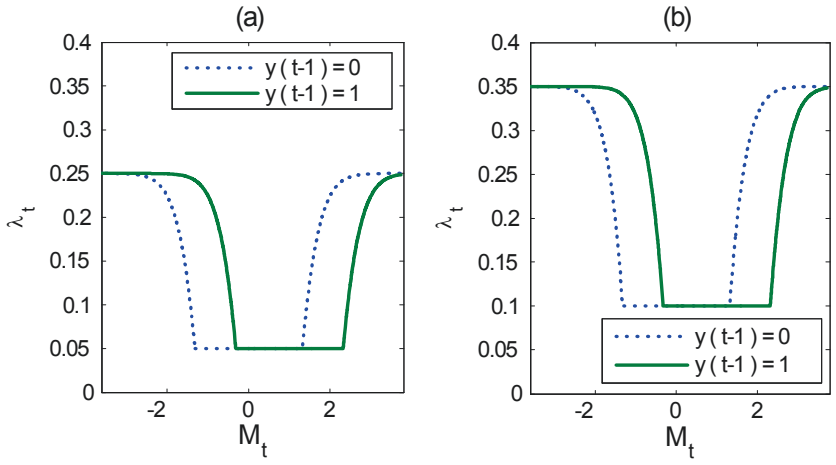

Figure 3: (a) Behavior of λ_t parameter in terms of M_t with $y_{t-1} = 0$ and $y_{t-1} = 1$ for AEWMA2-S^2 design with PS2: $\lambda_{\min} = 0.05$, $\lambda_{\max} = 0.25$, $a = 1$, $p_0 = 0.9$, $h = 0.1503$. (b) Behavior of λ_t parameter in terms of behavior M_t with $y_{t-1} = 0$ and $y_{t-1} = 1$ for AEWMA2-S^2 design with PS3: $\lambda_{\min} = 0.1$, $\lambda_{\max} = 0.35$, $a = 1$, $p_0 = 0.9$ and $h = 0.2572$.

3.3 The AEWMA3-S^2 chart

This chart is a combination of the AEWMA1-S^2 and AEWMA2-S^2 charts in the sense that we consider the statistic T_{1t} or T_{2t}, which is more pessimistic with respect to the evidence of misadjustment, that is $T_{3t} = \max(T_{1t}, T_{2t})$. Consequently, the AEWMA3-S^2 chart uses the following time-varying smoothing parameter,

$$\lambda_{3t} = \max(\lambda_{1t}^{(3)}, \lambda_{2t}), \tag{16}$$

which corresponds to use the statistic T_{3t} in the transformation (15). Figure 4 illustrates how λ_{3t} varies as a function of M_t, with two particular parameter sets. Notice that the same parameter set is used for both smoothing factors, $\lambda_{1t}^{(3)}$ and λ_{2t}. Since the statistics T_{3t} also depend on y_{t-1}, two curves with different values of y_{t-1} are displayed.

3.4 Computation of the ARL by using a Markov chain approach

This section shows a procedure to compute the ARL of the AEWMA1-S^2, AEWMA2-S^2, and AEWMA3-S^2 charts using a Markov chain approach. Following the idea of Brook and Evans (1972), Lucas and Saccucci (1990), Capizzi and Masarotto (2003) or Shu (2008), we can approximate the value of ARL by discretizing the infinite-state transition probability matrix of the continuous-state Markov chain

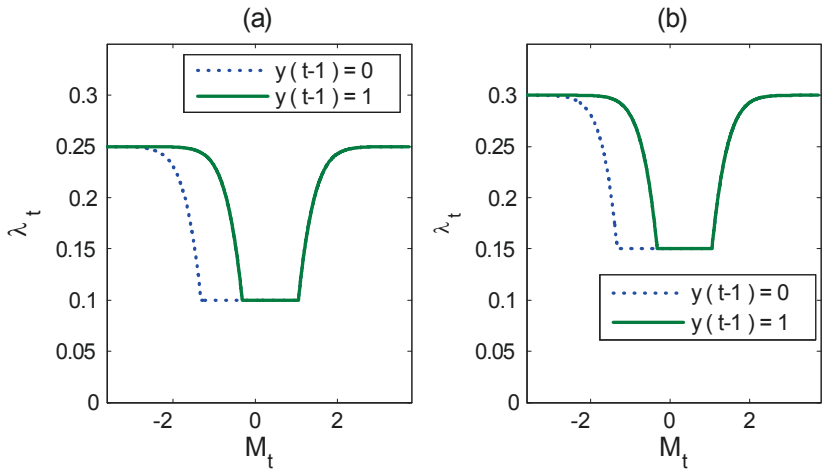

Figure 4: (a) Behavior of λ_t parameter in terms of M_t with $y_{t-1} = 0$ and $y_{t-1} = 1$ for an AEWMA3-S^2 design with PS4: $\lambda_{\min} = 0.1$, $\lambda_{\max} = 0.25$, $a = 1$, $p_0 = 0.9$, $h = 0.3023$. (b) Behavior of λ_t parameter in terms of behavior M_t with $y_{t-1} = 0$ and $y_{t-1} = 1$ for an AEMWA3-S^2 design with PS5: $\lambda_{\min} = 0.15$, $\lambda_{\max} = 0.3$, $a = 1$, $p_0 = 0.9$ and $h = 0.3855$.

defined by (7). For convenience, we rewrite the control statistics of the AEWMA-S^2 as,

$$y_t = \max\left[0, y_{t-1} + (M_t - y_{t-1})\,\lambda_t\right]. \tag{17}$$

The procedure consists in dividing the interval $[0, h]$ in an odd number m of subintervals Ω_j, $j = 1, 2, ..., m$. These subintervals have width $\omega = (2h)\,/\,(2m-1)$, except the first subinterval whose width is $\omega/2$. Each subinterval Ω_j, that represents the $j-$th state, has as midpoint $\nu_j = (j-1)\,\omega$. The control statistic y_t is considered to be in the transient state or subinterval Ω_j, at time t, if $\nu_j - \omega/2 < y_t < \nu_j + \omega/2$. Furthermore, y_t falls in an absorbing state when it exceeds a threshold h or 0. Let $P(j,k)$ be the transition probability of y_t of going from state j to state k. Then, for $j = 1, 2, 3, ..., m$ and $k \neq 1$,

$$\begin{aligned} P(j,k) &= \Pr\left(y_t \in \Omega_k \mid y_{t-1} \in \Omega_j\right) \qquad (18)\\ &= \Pr(\,v_k - \omega/2 < y_t \leq v_k + \omega/2 \mid\ y_{t-1} = v_j)\\ &= \Pr((k-1)\,\omega - \omega/2 < v_j + (M_t - v_j)\,\lambda_t \leq (k-1)\,\omega + \omega/2)\\ &= \Pr((k-1)\,\omega - \omega/2 - (j-1)\,\omega < (M_t - v_j)\,\lambda_t \leq (k-1)\,\omega + \omega/2 - (j-1)\,\omega)\\ &= \Pr((k-j-1/2)\,\omega < (M_t - v_j)\,\lambda_t \leq (k-j+1/2)\,\omega). \qquad (19) \end{aligned}$$

Let denote $a_1 = (k-j-1/2)\,\omega$ and $a_2 = (k-j+1/2)\,\omega$. Then,

$$\begin{aligned} P(j,k) &= \Pr\left[\exp(a_1) < \exp\left[\lambda_t\,(M_t - v_j)\right] \leq \exp(a_2)\right]\\ &= \Pr\left[\exp(a_1) < \frac{\exp(\lambda_t M_t)}{\exp(\lambda_t v_j)} \leq \exp(a_2)\right]. \qquad (20) \end{aligned}$$

Note that when $k = 1$,

$$P(j,1) = \Pr\left[\frac{\exp(\lambda_t M_t)}{\exp(\lambda_t v_j)} \leq \exp(a_2)\right].$$

Replacing $M_t = \ln\left(S_t^2/\sigma_0^2\right)$ in (20),

$$\begin{aligned} P(j,k) &= \Pr\left[\exp(a_1) < \frac{\exp\left[\lambda_t \ln\left(S_t^2/\sigma_0^2\right)\right]}{\exp(\lambda_t v_j)} \leq \exp(a_2)\right] \\ &= \Pr\left[\exp(a_1) < \frac{\left(S_t^2/\sigma_0^2\right)^{\lambda_t}}{\exp(\lambda_t v_j)} \leq \exp(a_2)\right]. \end{aligned} \tag{21}$$

The expression $\left(S_t^2/\sigma_0^2\right)^{\lambda_t}/\exp(\lambda_t v_j)$ in (21) does not have a trivial distribution since λ_t depends on $\left(S_t^2/\sigma_0^2\right)$ by (12), (15) or (16). Therefore, an approximation to the distribution is proposed. In this regard, it is known that $S_t^2/\sigma_0^2 \sim \Gamma\left((n-1)/2, 2\sigma^2/\left[(n-1)\sigma_0^2\right]\right)$. Let σ_S be the standard deviation of the random variable S_t^2/σ_0^2, then, it is known that,

$$\sigma_S = \left([(n-1)/2]\left[2\sigma^2/\left[(n-1)\sigma_0^2\right]\right]^2\right)^{1/2}. \tag{22}$$

Based on (22), a suitable probability interval for S_t^2/σ_0^2 is defined, for example, $(0, 7\sigma_S]$, since probability of falling above $7\sigma_S$ is very close to zero. The mentioned interval is discretized in m subintervals Ψ_i, $i = 1, 2, 3, ..., m$. Similarly to the previous discretization, the width of the subintervals is defined by $\varepsilon = 7\sigma_S/(2m-1)$ and the midpoint of $i-$th subinterval Ψ_i is denoted by u_i. If $S_t^2/\sigma_0^2 \in \Psi_i$ then $u_i - \varepsilon/2 < S_t^2/\sigma_0^2 \leq u_i + \varepsilon/2$. In each of these subintervals, we approximate S_t^2/σ_0^2 to the value u_i. The approximate values for S_t^2/σ_0^2 can be used to assign an approximate value to M_t and λ_t in each subinterval as,

$$T_{1t} \approx \left(\frac{\ln u_i - \mu_{M0}}{\sigma_M}\right)^2 \equiv c_i \quad \text{or} \quad T_{2t} \approx \left(\frac{\ln u_i - v_j}{\sigma_M}\right)^2 \equiv c_i \quad \text{or} \quad T_{3t} \approx \max(T_{1t}, T_{2t}) \equiv c_i$$

$$\begin{aligned} r_i &= P\left(\chi_1^2 < c_i\right) \\ q_i &= \begin{cases} 0 & \text{if} \quad r_i^a \leq p_0, \\ \dfrac{r_i^a - p_0}{1 - p_0} & \text{otherwise}, \end{cases} \\ \lambda_i &= \lambda_{\min} + (\lambda_{\max} - \lambda_{\min})\, q_i. \end{aligned}$$

In consequence, if we want to approximate the values of $P(j,k)$ in (18), we can condition on each subinterval Ψ_i and apply the total probability formula as,

$$\begin{aligned} P(j,k) &= \Pr\left[\exp(a_1) \leq \frac{\left(S_t^2/\sigma_0^2\right)^{\lambda_t}}{\exp(\lambda_t v_j)} \leq \exp(a_2)\right] \\ &= \sum_{i=1}^{m} \Pr\left[\exp(a_1) \leq \frac{\left(S_t^2/\sigma_0^2\right)^{\lambda_t}}{\exp(\lambda_t v_j)} \leq \exp(a_2) \;\middle|\; S_t^2/\sigma_0^2 \in \Psi_i\right] \Pr\left[S_t^2/\sigma_0^2 \in \Psi_i\right] \\ &\approx \sum_{i=1}^{m} \Pr\left[\exp(a_1) \leq \frac{(u_i)^{\lambda_i}}{\exp(\lambda_i v_j)} \leq \exp(a_2)\right] \Pr\left[S_t^2/\sigma_0^2 \in \Psi_i\right]. \end{aligned} \tag{23}$$

Notice that since u_i is a constant in each subinterval, the first probability at the right hand side of (23) is easy to compute, since it is just 1 or 0. The second one is also easy to compute, since we have that $S_t^2/\sigma_0^2 \sim \Gamma\left((n-1)/2, 2\sigma^2/\left[(n-1)\sigma_0^2\right]\right)$. Finally, let $\mathbf{R}_{m\times m}$ be a submatrix that contains the probabilities $P(j,k)$ of going from the transient state j to the state k, $\mathbf{p}_{ini}$ is an initial probability vector of the states, $\mathbf{I}$ is the $m \times m$ identity matrix, and $\mathbf{1}$ is a $m \times 1$ vector of ones. Then, the probability function of RL and hence the ARL in zero-state, are given by,

$$\Pr(RL = rl) = \mathbf{p}'_{ini}\left(\mathbf{R}^{rl-1} - \mathbf{R}^{t}\right)\mathbf{1},$$

and

$$ARL = \mathbf{p}'_{ini}\left(\mathbf{I} - \mathbf{R}\right)^{-1}\mathbf{1}, \tag{24}$$

respectively. Lucas and Saccucci (1990) or Shu (2008) suggest for calculating the ARL in steady-state, using cyclic probability vector steady-state, $\mathbf{p}_{ss}$, which is obtained by solving $\mathbf{p}_{ss} = \mathbf{P}'_1\mathbf{p}_{ss}$, subject to $\mathbf{1}'\mathbf{p}_{ss} = 1$, where $\mathbf{P}_1$ is the ergodic transition probability matrix defined by,

$$\mathbf{P}_1 = \begin{pmatrix} \mathbf{R} & (\mathbf{I}-\mathbf{R})\mathbf{1} \\ 1\ 0\ 0 \ldots 0 & 0 \end{pmatrix}.$$

Hence, the steady-state ARL is obtained by,

$$ARL = \mathbf{q}'\left(\mathbf{I} - \mathbf{R}\right)^{-1}\mathbf{1}, \tag{25}$$

where, $\mathbf{q}$ is a vector of length m obtained from $\mathbf{p}_{ss}$ by deleting the entry corresponding to the absorbing state and normalizing so that the probabilities sum to 1.

Finally, for a given ARL_0 value and a rational subgroup of size n, the following optimization nonlinear problem with decision variables: $\lambda_{\min}, \lambda_{\max}, a, p_0$, and h, should be solved by,

$$\begin{aligned} &\min_{\lambda_{\min},\lambda_{\max},a,p_0,h} f\left(ARL\left(\tau(i)\right)\right), i = 1,2,\ldots,k. \\ \text{subject to:} \quad & \\ &ARL\left(\tau = 1, \lambda_{\min}, \lambda_{\max}, a, p_0, h\right) = ARL_0 \end{aligned}, \tag{26}$$

where $f(\cdot) : \mathbb{R}^k \to \mathbb{R}$, can be $\sum_{i=1}^{k} ARL\left(\tau(i)\right)$, the norm $\left\|ARL\left(\tau(i)\right)\right\|_2$, or some other convenient function, which is defined by the suitable optimality criteria. In this work, we are using the Euclidean distance between the vectors $\left[ARL\left(\tau(1)\right), ARL\left(\tau(2)\right), \ldots, ARL\left(\tau(k)\right)\right]$ and $\left[ARL^*\left(\tau(1)\right), ARL^*\left(\tau(2)\right), \ldots, ARL^*\left(\tau(
where $ARL^*(i)$ is the corresponding ARL^* shown in Table 1. That function is simple and has a good performance. Hence, the $ARL\left(\tau(i), \lambda_{\min}, \lambda_{\max}, a, p_0, h\right)$ is approximated by using the Markov Chain approach assuming $X_t \sim N(\mu_0, \tau^2\sigma^2)$.

	AEWMA1-S²-1	**AEWMA2-S²-1**	**AEWMA3-S²-1**	**AEWMA1-S²-2**	**AEWMA2-S²-2**	**AEWMA3-S²-2**
$\lambda_{\min}$	0.0632	0.0277	0.0769	0.4455	0.5949	0.0256
$\lambda_{\max}$	0.1115	0.0787	0.1399	0.7063	1.0000	0.6876
a	2.3458	4.0097	8.5720	6.6610	0.2746	2.2590
p_0	0.3584	0.0278	0.5060	0.1463	0.9747	0.4016
h	0.2225	0.1188	0.2062	0.8834	0.8866	0.8146

Table 2: Optimal parameters of the AEWMA-S^2 control chart designs in zero-state, $ARL_0 = 200$ and $n = 5$.

	AEWMA1-S²-1	**AEWMA2-S²-1**	**AEWMA3-S²-1**	**AEWMA1-S²-2**	**AEWMA2-S²-2**	**AEWMA3-S²-2**
$\lambda_{\min}$	0.0181	0.0145	0.0385	0.1737	0.2042	0.2000
$\lambda_{\max}$	0.2249	0.7524	0.2510	0.3625	0.2921	0.3111
a	7.5594	7.2188	7.8067	5.6608	0.1474	9.7789
p_0	0.8866	0.7570	0.8832	0.5923	0.9579	0.1138
h	0.0546	0.0445	0.1085	0.4226	0.4401	0.4579

Table 3: Optimal parameters of the AEWMA-S^2 control chart designs in steady-state, $ARL_0 = 200$ and $n = 5$.

Six alternative designs have been considered in zero-state process control, for an $ARL_0 = 200$, a rational subgroup of size $n = 5$ and λ defined by (12), (15) or (16). The first three use the following optimality criteria: minimizing the ARL at range of shifts $[1.1, 2]$, these designs are denoted by AEWMA1-S^2-1, AEWMA2–S^2-1 and AEWMA3-S^2-1. The others three use the optimality criteria: minimizing the ARL at range of shifts $[1.6, 3]$ and these are denoted by AEWMA1-S^2-2, AEWMA2-S^2-2 and AEWMA3-S^2-2.

Table 2 shows the optimal parameter values of the AEWMA-S^2 charts for the zero-state case. Similarly, Table 3 shows the optimal parameter values, in the steady-state case. In this paper, for simplicity, and without loss of generality, the ARL values are computed assuming that $\mu_0 = 0$ and $\sigma = 1$. Tables 4 and 5 show the ARL profiles for zero-state and steady-state, respectively, based on the optimal parameters.

4 Adaptive EWMA based on the value of the control statistics

In this AEWMA-S^2 chart, denoted as AEWMA4-S^2, λ_t is based on the value of y_{t-1}. It uses the following statistic

$$D_t = \left|\frac{y_{t-1}}{H}\right| = \left|\frac{y_{t-1}}{h}\right|,$$

which is the ratio between y_{t-1} and the control limit $H = h$. The closer y_{t-1} is to the control limit, the closer D_t to 1 is. Then, using (12) with $F_{1t} = D_t$ or (15) with $G_{2t} = D_t$, the misadjustment can be translated into a time-varying smoothing parameter λ_t. It should be noticed that statistic D_t does not depend on M_t, which makes easer the ARL calculation. Figure 5 shows the behavior of λ_t versus

τ	AEWMA1-S^2-1	AEWMA2-S^2-1	AEWMA3-S^2-1	AEWMA1-S^2-2	AEWMA2-S^2-2	AEWMA3-S^2-2
1.1	**41.79**	41.99	42.63	55.71	55.64	53.43
1.2	**17.19**	17.20	17.41	22.59	22.60	21.46
1.3	10.04	**9.91**	10.00	11.89	11.91	11.42
1.4	7.01	**6.82**	6.87	7.46	7.47	7.28
1.5	5.40	**5.18**	5.22	5.28	5.28	5.21
1.6	4.43	4.18	4.22	4.05	4.05	**4.03**
1.7	3.78	3.52	3.55	**3.28**	**3.28**	**3.28**
2.0	2.71	2.43	2.45	**2.16**	**2.16**	**2.16**
2.5	1.95	1.70	1.71	**1.51**	**1.51**	**1.51**
3.0	1.58	1.39	1.40	**1.27**	**1.27**	**1.27**

Table 4: The ARL values in zero-state with $ARL_0 = 200$ and $n = 5$.

τ	AEWMA1-S^2-1	AEWMA2-S^2-1	AEWMA3-S^2-1	AEWMA1-S^2-2	AEWMA2-S^2-2	AEWMA3-S^2-2
1.1	37.33	**37.33**	38.32	46.06	45.11	44.99
1.2	**14.38**	14.43	14.67	17.30	17.03	16.95
1.3	**8.10**	8.14	8.16	9.03	8.92	8.88
1.4	5.60	5.63	**5.58**	5.81	5.74	5.72
1.5	4.34	4.36	**4.29**	4.25	4.21	4.20
1.6	3.59	3.61	3.54	3.38	3.35	**3.34**
1.7	3.10	3.12	3.05	2.84	2.82	**2.81**
2.0	2.30	2.31	2.25	**2.01**	2.02	**2.01**
2.5	1.70	1.71	1.68	**1.49**	1.52	1.52
3	1.41	1.41	1.40	**1.28**	1.30	1.30

Table 5: The ARL values in steady-state with $ARL_0 = 200$ and $n = 5$.

D_t for two AEWMA4-S^2 designs (D-1 and D-2). When the process is out of control, λ_t tends to take the highest possible value.

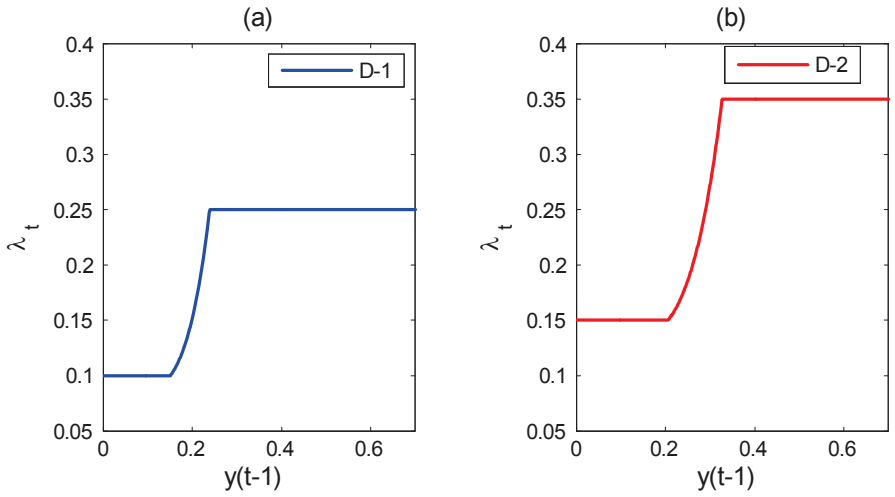

Figure 5: (a) Behavior of λ_t parameter in terms of y_{t-1} for an AEWMA4-S^2 control chart design D-1 with PS6: $\lambda_{\min} = 0.1$, $\lambda_{\max} = 0.25$, $a = 5$, $p_0 = 0.1$, $h = 0.23912$. (b) Behavior of λ_t parameter in terms of behavior y_{t-1} for an AEMWA4-S^2 control chart design D-2 with PS7: $\lambda_{\min} = 0.15$, $\lambda_{\max} = 0.35$, $a = 5$, $p_0 = 0.1$ and $h = 0.327$.

4.1 Computation of the ARL of the AEWMA4-S^2 using a Markov chain approach

In this AEWMA-S^2 chart, λ_t does not depend on M_t. The computation of the ARL follows the traditional procedure proposed by Brook and Evans (1972) and Lucas and Saccucci (1990). The transition probability defined in (19) can be reexpressed as follows

$$\begin{aligned} P(j,k) &= \Pr\left[\nu_k - \nu_j - \omega/2 \leq (M_t - \nu_j)\lambda_t \leq \nu_k - \nu_j + \omega/2\right] \\ &= \Pr\left[\frac{\nu_k - \nu_j - \omega/2}{\lambda_t} - \nu_j \leq M_t \leq \frac{\nu_k - \nu_j + \omega/2}{\lambda_t} - \nu_j\right] \\ &= \Pr\left[\exp(b_1) < \exp(M_t) \leq \exp(b_2)\right] \\ &= \Pr\left[\exp(b_1) < S_t^2/\sigma_0^2 \leq \exp(b_2)\right], \end{aligned} \tag{27}$$

where, $b_1 = (\nu_k - \nu_j - \omega/2)/\lambda_t - \nu_j$, $b_2 = (\nu_k - \nu_j + \omega/2)/\lambda_t - \nu_j$. The probability (27) is computed using that $S_t^2/\sigma_0^2 \sim \Gamma\left((n-1)/2, 2\sigma^2/\left[(n-1)\sigma_0^2\right]\right)$. The ARL is calculated in zero-state or steady-state by (24) and (25), respectively. Finally, solving the nonlinear optimization problem (26), the optimal values of the parameters can be obtained.

For a zero-state process control and $ARL_0 = 200$, rational subgroup of size $n = 5$ and using (12) with $F_{1t} = D_t$, two designs are obtained. The first one uses the following optimality criteria:

	$ARL_0 = 200$, zero-state		$ARL_0 = 200$, steady-state	
	AEWMA4-S^2-1	**AEWMA4-S^2-2**	**AEWMA4-S^2-1**	**AEWMA4-S^2-2**
$\lambda_{\min}$	0.0886	0.6197	0.0821	0.2719
$\lambda_{\max}$	0.5863	0.6697	0.1121	0.6444
a	9.4988	3.8766	5.1453	6.1695
p_0	0.9983	0.2326	0.2222	0.9949
h	0.2182	0.8966	0.2059	0.5043

Table 6: Optimal parameters of the AEWMA-S^2 control chart designs.

	$ARL_0 = 200$, zero-state		$ARL_0 = 200$, steady-state	
τ	**AEWMA4-S^2-1**	**AEWMA4-S^2-2**	**AEWMA4-S^2-1**	**AEWMA4-S^2-2**
1.1	**43.96**	55.09	**41.25**	46.34
1.2	**18.19**	22.40	**15.67**	17.67
1.3	**10.60**	11.84	**8.52**	9.25
1.4	**7.41**	7.46	**5.71**	5.93
1.5	5.74	**5.29**	**4.33**	**4.33**
1.6	4.74	**4.07**	3.54	**3.44**
1.7	4.08	**3.31**	3.04	**2.89**
2	3.00	**2.19**	2.27	**2.08**
2.5	2.25	**1.54**	1.78	**1.59**
3	1.87	**1.29**	1.56	**1.38**

Table 7: The ARL values with $n = 5$.

minimizing the ARL at range of shifts $[1.1, 2]$, this design is denoted by AEWMA4-S^2-1 control chart design. The other one uses the optimality criteria: minimizing the ARL at range of shifts $[1.6, 3]$ and this is denoted by AEWMA4-S^2-2 control chart design. The optimal values of parameters are shown in Table 6. The ARL profiles are shown in the Table 7.

5 Comparisons

In this section, the four proposed AEWMA-S^2 control charts are compared. Besides, they are compared to other control charts such as Shewhart-S^2 control chart, the EWMA-S^2 control charts, the EWMA-S^2 of Castagliola et al (2010) called here EWMA-S^2-CT and the adaptive EWMA control charts for the variance of Shu (2008) called here AEWMA-S^2-SH. Unless otherwise stated, all the comparisons consider: zero-state ARL, $ARL_0 = 200$ and $n = 5$.

Table 8 shows that the performance of the four proposed AEWMA-S^2 charts are similar for small and medium shifts in approximately the range $[1.1, 1.4]$. The AEWMA1-S^2-1 design shows a slightly better performance than the others. In the interval $1.4 < \tau < 3$, the first three AEWMA-S^2 designs show similar performance, being again the first one slightly better than the others. The AEWMA4-S^2-1

design loses efficiency for medium and large shifts.

On the other hand, Table 8 shows that also the four AEWMA-S^2 designs have similar performance for small and medium shifts in the variance process, approximately $1.1 \leq \tau \leq 1.5$. The AEWMA3-S^2-2 design is slightly better than the others for very small and medium shifts, $\tau \in [1.1, 1.6]$. In the interval $\tau \in [1.7, 3]$, the first three AEWMA-S^2 designs show similar performance. The AEWMA4-S^2-2 design loses efficiency for medium and large shifts.

In Table 8 , we can compare the first four AEWMA-S^2 designs and a Shewhart-S^2 control chart with the same rational subgroup size, $n = 5$ (S-1 design). It can be seen that Shewhart control chart is not competitive for small and medium shifts. Also, we can compare the second four AEWMA-S^2 charts and the same Shewhart-S^2 design (S-1). In this case, S-1 is still less competitive than four AEWMA-S^2 designs.

Besides, we can compare the ARL values of the first four AEWMA-S^2 designs and two alternative EWMA-S^2 designs. These EWMA-S^2 charts are designed to get minimum ARL values at shifts $\tau = 1.1$ (E-1) and $\tau = 1.5$ (E-2). In this case, it can be seen that the four proposed AEWMA-S^2 designs and only E-1 have a similar performance for small shifts, E-1 is only competitive in $\tau = 1.1$. E-2 is not competitive for small and medium shifts. For large shifts, approximately $\tau \geq 1.5$, the first three AEWMA-S^2 designs are competitive with E-2 but E-1 is not competitive. Definitely, the four proposed AEWMA-S^2 control charts show good performance through the whole shifts range. Additionally, we can compare the ARL values of the second four AEWMA-S^2 charts and the EWMA-S^2 with designs that were got for minimum ARL values at shifts $\tau = 2$ (E-3) and $\tau = 3$ (E-4). In this case, it can be seen that the four proposed AEWMA-S^2 designs have good performance for every possible shifts, E-3 and E-4 are only competitive for $\tau \geq 2.5$.

Moreover, Table 8 allows us to compare the ARL values of the first four AEWMA-S^2 designs with two alternative EWMA-S^2-CT charts. These EWMA-S^2-CT charts are designed to get minimum ARL values at shifts $\tau = 1.1$ (CT-1) and $\tau = 1.5$ (CT-2). This comparison shows that the four proposed AEWMA-S^2 control charts are more competitive than CT-1 and CT-2 for approximately $\tau \leq 1.5$. Only CT-2 is competitive in $\tau \geq 1.6$. Furthermore, we can compare the ARL values of the second four AEWMA-S^2 charts and the EWMA-S^2-CT charts for two design, with minimum ARL values at shifts $\tau = 2$ (CT-3) and $\tau = 3$ (CT-4). In this case, it can be seen that the four proposed AEWMA-S^2 control charts have a competitive performance for all shift, CT-3 and CT-4 are only competitive for $\tau \geq 2.5$.

Our final comparison is between the proposed AEWMA-S^2 control charts and the AEWMA-S^2 control charts of Shu (2008). In this regard, Table 8 allows us to compare the first four proposed

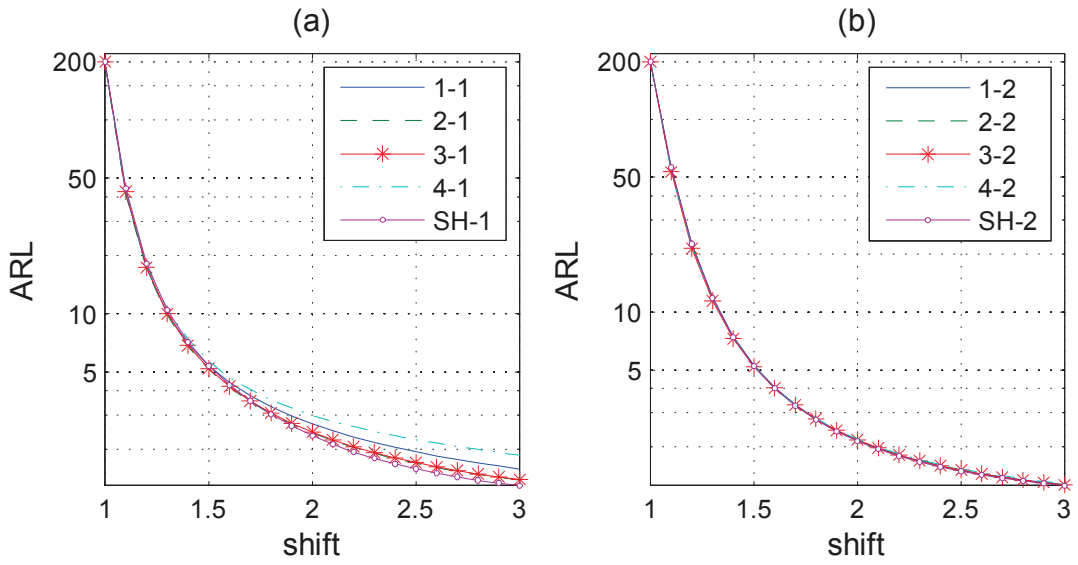

Figure 6: (a) *ARL* comparisons between four AEWMA-S^2 designs proposed, AEWMA-S^2-(1-1, 2-1, 3-1 and 4-1) and AEWMA-S^2-SH-1. (b) *ARL* comparisons between four AEWMA-S^2 designs proposed, AEWMA-S^2-(1-2, 2-2, 3-2 and 4-2) and AEWMA-S^2-SH-2. For $ARL_0 = 200$ and $n = 5$.

AEWMA-S^2 control charts (designs optimized for $\tau \in [1.1, 2]$ as in Shu, 2008) with the AEWMA-S^2-SH-1 (design optimized for $\tau \in [1.1, 2]$ as in Shu, 2008) based on the Huber score function. This design is labelled as SH-1. The first three proposed AEWMA-S^2 are better than SH-1 for small and medium shifts, approximately for $\tau \in [1.1, 1.6]$. Then, for large shifts, these designs are similar, being AEWMA4-S^2-1 less competitive.

Finally, in table 8 we can compare the second four proposed AEWMA-S^2 control charts (designs optimized for $\tau \in [1.6, 3]$ as it was mentioned in the previous section) with the AEWMA-S^2-SH-2 (design optimized for $\tau \in [1.4, 2]$ as it was mentioned in Shu, 2008) based on the Huber score function. This design is labelled as SH-2. In general, again, it can be seen that the ARL of the four proposed AEWMA-S^2 designs and SH-2 are similar in almost all range of shifts. The four AEWMA-S^2 proposed take advantage of SH-2 for small and medium shifts, approximately for $\tau \in [1.1, 1.5]$. Then, for large shifts, the five designs are similar. Therefore, it can be concluded that the proposed AEWMA-S^2 control chart are more competitive than the AEWMA-S^2-SH in terms of ARL particularly for small and medium shifts. Figure 6 shows the final comparisons.

6 Conclusions

We have presented four adaptive EWMA control charts for monitoring the variance of a variable that represents a quality characteristic in a particular process. These control charts work with a time

	τ									
	1.1	**1.2**	**1.3**	**1.4**	**1.5**	**1.6**	**1.7**	**2.0**	**2.5**	**3.0**
1-S^2-1	41.79	17.19	10.04	7.01	5.40	4.43	3.78	2.71	1.95	1.58
2-S^2-1	41.99	17.20	9.91	6.82	5.18	4.18	3.52	2.43	1.70	1.39
3-S^2-1	42.63	17.41	10.00	6.87	5.22	4.22	3.55	2.45	1.71	1.40
4-S^2-1	43.96	18.19	10.60	7.41	5.74	4.74	4.08	3.00	2.25	1.87
1-S^2-2	55.71	22.59	11.89	7.46	5.28	4.05	3.28	2.16	1.51	1.27
2-S^2-2	55.64	22.60	11.91	7.47	5.28	4.05	3.28	2.16	1.51	1.27
3-S^2-2	53.43	21.46	11.42	7.28	5.21	4.03	3.28	2.16	1.51	1.27
4-S^2-2	55.09	22.40	11.84	7.46	5.29	4.07	3.31	2.19	1.54	1.29
S-1	95.15	42.39	21.58	12.61	8.24	5.86	4.46	2.55	1.61	1.30
E-1	41.98	18.19	11.13	8.06	6.40	5.37	4.67	3.48	2.64	2.26
E-2	51.41	20.64	11.07	7.14	5.18	4.06	3.35	2.29	1.62	1.34
E-3	58.11	24.00	12.64	7.87	5.50	4.17	3.36	2.17	1.51	1.27
E-4	65.03	28.27	15.04	9.25	6.32	4.67	3.66	2.24	1.50	1.25
CT-1	46.33	20.64	13.17	9.73	7.76	6.48	5.58	3.96	2.67	2.03
CT-2	58.98	22.47	11.66	7.39	5.30	4.13	3.39	2.28	1.60	1.33
CT-3	60.70	24.91	12.99	8.02	5.57	4.20	3.36	2.16	1.49	1.26
CT-4	65.02	28.27	15.04	9.25	6.32	4.67	3.66	2.24	1.50	1.25
SH-1	44.37	18.20	10.48	7.17	5.39	4.29	3.55	2.35	1.59	1.30
SH-2	56.41	22.63	11.81	7.40	5.23	4.01	3.26	2.14	1.49	1.25

Table 8: The ARL values in zero-state with $ARL_0 = 200$ and $n = 5$. We are considered: AEWMA1-S^2-1 (1-S^2-1), AEWMA2-S^2-1 (2-S^2-1), AEWMA3-S^2-1 (3-S^2-1), AEWMA4-S^2-1 (4-S^2-1), AEWMA1-S^2-2 (1-S^2-2), AEWMA2-S^2-2 (2-S^2-2), AEWMA3-S^2-2 (3-S^2-2), AEWMA4-S^2-2 (4-S^2-2), Shewhart-S^2 (S-1), EWMA-S^2-1 (E-1), EWMA-S^2-2 (E-2), EWMA-S^2-3 (E-3), EWMA-S^2-4 (E-4), EWMA-S^2-CT1 (CT-1), EWMA-S^2-CT2 (CT-2), EWMA-S^2-CT3 (CT-3), EWMA-S^2-CT4 (CT-4), AEWMA-S^2-SH-1 (SH-1) and AEWMA-S^2-SH-2 (SH-2).

varying smoothing parameter. The proposed AEWMA-S^2 control charts are very easy to understand and to implement in the practice. We should have in mind that the size shift depends on the nature of the monitored process. Since in actual operation, smaller shifts are more frequent than larger shifts, we have shown that these proposed charts have a good performance for small and medium shifts and even for large shifts. Therefore, the proposed charts can be competitive with respect to the alternative charts of the literature on a wide range of shifts.

6.0.1 Acknowledgements

The financial support received from the Spanish MEC, under grant ECO2012-38442 is gratefully acknowledge.

References

[1] Abbasi, S. A. (2010). On sensitivity of EWMA control chart for monitoring process dispersion. In Proceedings of the World Congress on Engineering, 3, 2027-2032.

[2] Abbasi, S. A. and Miller, A. (2013). MDEWMA chart: an efficient and robust alternative to monitor process dispersion. Journal of Statistical Computation and Simulation, 83(2), 247-268.

[3] Acosta-Mejia, C. A. (1998). Monitoring reduction in variability with the range. IIE transactions, 30(6), 515-523.

[4] Acosta-Mejia, C. A., Pignatiello, J. J. and Rao, B. V. (1999). A comparison of control charting procedures for monitoring process dispersion. IIE transactions, 31(6), 569-579.

[5] Amin, R. W., Wolff, H., Besenfelder, W. and Baxley Jr, R. (1999). EWMA control charts for the smallest and largest observations. Journal of Quality Technology, 31(2), 189-201.

[6] Bagshaw, M. and Johnson, R. A. (1975). The effect of serial correlation on the performance of CUSUM tests II. Technometrics, 17(1), 73-80.

[7] Box, G. E., Hunter, W. G. and Hunter, J. S. (1978). Statistics for experimenters. John Wiley & Sons, New York, NY.

[8] Box, G. E. P. and Ramirez, J. G (1991a). Sequential Methods in Statistical Process Monitoring. Report No. 65, Center for Quality and Productivity Improvement, University of Wisconsin-Madison, Madison, WI.

[9] Box, G, E. P. and Ramirez, J. G. (1991b). Sequential Methods in Statistical Process Monitoring. Report No. 66, Center for Quality and Productivity Improvement, University of Wisconsin-Madison, Madison, WI.

[10] Box, G. E. P. and Ramirez, J. G. (1991c). Sequential Methods in Statistical Process Monitoring. Report No. 67, Center for Quality and Productivity Improvement, University of Wisconsin-Madison, Madison, WI.

[11] Brook D. and Evans D. A. (1972). An approach to the probability distribution of CUSUM run length. Biometrika, 59(3), 539-549.

[12] Capizzi G. and Masarotto G. (2003). An adaptive exponentially weighted moving average control chart. Technometrics, 45(3), 199-207.

[13] Castagliola, P. (2005). A New S2-EWMA Control Chart for Monitoring the Process Variance. Quality and Reliability Engineering International, 21(8), 781-794.

[14] Castagliola, P., Celano, G., Fichera, S. and Giuffrida, F. (2006). A variable sampling interval S^2-EWMA control chart for monitoring the process variance. International Journal of Technology Management, 37(1-2), 125-146.

[15] Castagliola, P., Celano, G., Fichera, S. and Nunnari, V. (2008). A variable sample size S^2-EWMA control chart for monitoring the process variance. International Journal of Reliability, Quality and Safety Engineering, 15(3), 181-201.

[16] Castagliola, P., Celano, G. and Fichera, S. (2009). A new CUSUM-S^2 control chart for monitoring the process variance. Journal of Quality in Maintenance Engineering, 15(4), 344-357.

[17] Castagliola, P., Celano, G. and Fichera, S. (2010). A Johnson's type transformation EWMA-S^2 control chart. International Journal of Quality Engineering and Technology, 1(3), 253-275.

[18] Chang, T. C. and Gan, F. F. (1995). Cumulative sum control chart for monitoring process variance. Journal of Quality Technology. 27(2), 109-119.

[19] Chao-Wen, L. and Reynolds Jr, M. R. (1999). Control charts for monitoring the mean and variance of autocorrelated process. Journal of Quality Technology, 31(3), 259-274.

[20] Chengular, I., Arnolds, J. and Reynolds, Jr., M.R. (1989). Variable sampling intervals for multiparameter Shewhart charts. Communications in Statistics: Theory and Methods, 18(5),.1769–1792.

[21] Crowder, S. V.and Hamilton, M. D. (1992). An EWMA for monitoring a process standard deviation. Journal of Quality Technology, 24(1), 12-21.

[22] Gan, F. F. (1995). Joint monitoring of process mean and variance using exponentially weighted moving average control charts. Technometrics, 37(4), 446-453.

[23] Haq, A., Brown, J. and Moltchanova, E. (2014). New exponentially weighted moving average control charts for monitoring process mean and process dispersion. Quality and Reliability Engineering International.

[24] Hawkins, D. M. (1981). A CUSUM for a scale parameter. Journal of Quality Technology, 13(4), 228-231.

[25] Huber P. J. (1981). Robust statistics. New York: Wiley.

[26] Huwang, L., Huang, C. J. and Wang, Y. H. T. (2010). New EWMA control charts for monitoring process dispersion. Computational Statistics & Data Analysis, 54(10), 2328-2342.

[27] Johnson, N. L. (1949). Systems of frequency curves generated by methods of translation. Biometrika, 36(1-2), 149-176.

[28] Lowry, C. A., Champ, C. W. and Woodall, W. H. (1995). The performance of control charts for monitoring process variation. Communications in Statistics-Simulation and Computation, 24(2), 409-437.

[29] Lucas J. M. and Saccucci M. S. (1990). Exponentially weighted moving average control schemes: Properties and Enhancements (with discussion), Technometrics, 32(1), pp. 1-29.

[30] MacGregor, J. F. and Harris, T. J. (1993). The exponentially weighted moving variance. Journal of Quality Technology, 25(2), 106-118.

[31] Maravelakis, P. E. and Castagliola, P. (2009). An EWMA chart for monitoring the process standard deviation when parameters are estimated. Computational Statistics & Data Analysis, 53(7), 2653-2664.

[32] Nazir, H. Z., Riaz, M. and Does, R. J. (2015). Robust CUSUM control charting for process dispersion. Quality and Reliability Engineering International, 31(3), 369-379.

[33] Ng, C. H. and Case, K. E. (1989). Development and evaluation of control charts using exponentially weighted moving averages. Journal of Quality Technology, 21(4), 242-250.

[34] Page, E. S. (1963). Controlling the standard deviation by CUSUMS and warning lines. Technometrics, 5(3), 307-315.

[35] Reynolds Jr., M. R. and Stoumbos, Z. (2001). Monitoring the process mean and variance using individual observations and variable sampling intervals. Journal of Quality Technology, 33(2), 181-205.

[36] Sánchez, I. (2006). Recursive estimation of dynamic models using Cook's distance, with application to wind energy forecast. Technometrics, 48(1), 61-73.

[37] Shewhart W. A. (1931). Economic control of quality of manufactured product. D. Van Nostrand Company, Inc, The United States of America, 182.

[38] Shu, L. (2008). An adaptive exponentially weighted moving average control chart for monitoring process variances. Journal of Statistical Computation and Simulation, 78(4), 367-384.

[39] Shu, L. and Jiang, W. (2008). A new EWMA chart for monitoring process dispersion. Journal of Quality Technology, 40(3), 319-331.

[40] Shu, L., Yeung, H. F. and Jiang, W. (2010). An adaptive CUSUM procedure for signaling process variance changes of unknown sizes. Journal of Quality Technology, 42(1), 69.

[41] Sparks, R. S. (2000). CUSUM Charts for Signaling Varying Location Shifts. Journal of Quality Technology 32(2), 157-171.

[42] Sweet, A. L. (1986). Control charts using coupled exponentially weighted moving averages. IIE Transactions, 18(1), 26-33.

[43] Tuprah, K. and Ncube, M. (1987). A comparison of dispersion quality control charts. Sequential Analysis, 6(2), 155-163.

[44] Ugaz, W., Sánchez, I. and Alonso, A. M. (2016). Adaptive EWMA Control Charts with a Time Varying Smoothing Parameter. Preprint.

[45] Wortham, A. W. and Ringer, L. J. (1971). Control via exponential smoothing. The Logistics Review, 7(32), 33-40.

[46] Yashchin, E. (1995). Estimating the current mean of a process subject to abrupt changes. Technometrics, 37(3), 311–323.